Int. J. Electrochem. Sci., 17 **(2022)** Article Number: 221049, doi: 10.20964/2022.10.54

International Journal of
ELECTROCHEMICAL
SCIENCE
www.electrochemsci.org

Preparation and Electrochemical Properties of Conjugated Polymers with Carbazole Unit as Side Chain Terminal Group for Supercapacitor Electrodes

Huijun Zhang, Guanqun Zhu, Pengna Wang, Xuan Zhao, Xueqin Zhang, Ying Sun and Hong Yang**

School of Chemistry and Chemical Engineering, Southeast University, Nanjing 211189, China.
*E-mail: sunyseu@seu.edu.cn, yangh@seu.edu.cn.

Received: 14 June 2022 / *Accepted:* 21 August 2022 / *Published:* 10 September 2022

An electrochromic supercapacitor (ESC) not only has energy storage properties but also directly indicates the energy storage level by the colour difference at various applied voltages. Electropolymerization of active monomers can provide polymer films with porous structures for electrode materials with both electrochemical properties and electrochromic properties. However, the low molecular weight and undefined structure of the electropolymerized film, as well as the related electrode defects, limit its application in an ESC. Employing conjugated polymer rather than the small molecule monomer as the initial electroactive moieties of the electropolymerization for ESC electrodes ensures the desirable conjugation length and relatively planar structure, which is expected to improve the conductivity and stability and hence the ESC performance. Here, we have designed and synthesized a novel conjugated polymer, PCZBDTCZ, with a side chain, terminal-modified carbazole group, which can be electrically polymerized to yield a crosslinked polymer film. Furthermore, different crosslinking agents have been introduced in the electropolymerization process, and seven new crosslinked conjugated polymer films have been prepared. The effects of cross-linking agents with different structures and mixed cross-linking agents on the morphology and electrochemical and electrochromic properties of the films were systematically investigated. The results indicated that the electropolymerization of the polymer PCZBDTCZ can produce electrode films with porous morphologies, and the loose pore structure can accelerate the transport of the electrolyte and shorten the response times of the materials, while the large-area cross-linked lattice structure can alleviate the volume change during cycling and hence improve the stability. Moreover, the crosslinked conjugated polymer PCZBDTCZ-D3P1-3 obtained by the introduction of two cross-linking agents had the best colouring efficiency and the maximum area ratio capacitance, demonstrating that tuning multiple crosslinking agents with excellent electrochemical active groups had a positive effect on the electrochemical and electrochromic properties of the materials.

Keywords Conjugated polymer, Crosslinking agent, Electropolymerization, Supercapacitor

1. INTRODUCTION

With scientific development, the demand for smart electronic products is gradually increasing. As one of the most important components in electronic devices, power systems have urgent requirements for their intelligent and flexible functions. Supercapacitors have already shown attractive superiority in their fast charging capability, high power density, long life duration and safe operation for practical application [1-7]. Electrochromism is defined as a phenomenon in which reversible and visible optical changes of a material occur consistent with charge injection and extraction during electrochemical oxidation or reduction [8,9]. Integrating electrochromism into a supercapacitor can fabricate an electrochromic supercapacitor (ESC), which indicates its charging state in real time by the colour change with the aid of a transparent conductive substrate. Hence, developing a bifunctional electrochromic supercapacitor with excellent electrochemical and electrochromic properties represents a promising way to develop smart power systems for wearable electronics, smart textiles, intelligent stealth, energy-storage smart windows and intelligent displays [10-15].

There are basically two kinds of electrode material candidates for ESC: metal oxides and conjugated polymers [16,17]. Due to the intrinsic drawbacks of metal oxides, such as slow switching times, intrinsic brittleness, low colouration efficiency and limited colour change range, significant research has focused on conjugated polymers with the advantages of rich colour range, high pseudocapacitance and fast switching [18-20]. More importantly, the polymer enables flexible and scaled up devices for various stationary and mobile applications.

However, most polymers typically suffer from low cycle stability, and consequently, capacitance decay will cause limited rate capability and lifetime, which will hinder practical applications. The instability of polymer film can be ascribed to the volume change of electrodes in doping/dedoping, leading to the generation of rupture during the charge injection and extraction process [21,22].

Formation of a well-defined porous and hollow structure has been expected to improve the cycle stability of electrode material, as severe volume change can be buffered and accommodated by the porous space [23]. More importantly, conductive polymers with porous structures have a larger specific surface area of electrochemical activity, which not only shortens the diffusion length of electrolyte ions but also increases the diffusion rate and accelerates the reaction kinetics [24].

The traditional method for building a porous structure in electrode material is to construct a covalent organic framework, which is simple to synthesize; however, the formation of a uniform film due to the initiative insolubility and poor dispersion is difficult [25]. In situ chemical polymerization is suitable for the preparation of electrode films, but the solution-coated film typically forms weak contact with the underlying substrate, causing substantial contact resistance and capacitance decay [26,27].

The electrochemical deposition technique functions as an effective way to obtain a porous film for ESC electrodes, as the film morphology can be well controlled and the porous structure can be manipulated [28]. Moreover, the film can typically be tightly adhered to the substrate, and consequently, a lower resistance contact can be obtained. Therefore, research attention has been given to the development of ESC electrodes with porous structures by electropolymerization.

Nevertheless, for the electropolymerized film of soluble monomers, a high molecular weight and specific structure are difficult to obtain, so severe inhomogeneity and defects may exist in the electrode,

leading to an undesirable influence on the conductivity and electrochemical properties. In addition, a loose morphology can always be formed in the electropolymerized film, and penetration of the electrolyte can probably cause mechanical looseness, which is detrimental to the long-term stability. Therefore, utilizing a conjugated polymer with a defined structure as the initial active material for electropolymerization can be a promising way to solve the above problems.

Significant studies have revealed that carbazole units can be electrically polymerized to obtain crosslinked structures [29]. Pan et al. discovered that doping crosslinkers with different structures, which can interact with conductive polymer chains to form stable networks, had a great impact on the morphology and electrochemical properties of conductive polymers [30].

Inspired by these works, we designed and synthesized a carbazole-based polymer, PCZBDTCZ, with side chain terminal-modified carbazole groups that can be electrically polymerized. Three crosslinking agents with different structures and mixed cross-linking agents were then introduced in electropolymerization to obtain seven novel, crosslinked polymer films with different surface morphologies and properties. By comparing the experimental results, we determined that the morphology and properties of crosslinked polymers were greatly influenced by different structures of crosslinking agents and electropolymerization methods. By electropolymerization, polymers with side chains attached to carbazole groups tend to obtain polymer films with porous structures. When the carbazole group on the side chain of PCZBDTCZ is electropolymerized with the carbazole group on the cross-linking agent, it is beneficial to form a looser structure and to accelerate the transport of electrolyte ions, showing a faster response time. The introduction of a three-branched, cross-linking agent with 3,4-ethylene dioxythiophene (EDOT) grafted at the end is more conducive to the formation of a larger-area, cross-linked lattice structure, which can effectively slow the volume change of the electrode material during cycling and improve the stability. Moreover, benefiting from the good synergistic effect of the two different cross-linking agents in the hybrid cross-linking agent, the cross-linked polymer films exhibited good optical contrast and excellent colouring efficiency, and the cycle performance was improved.

2. EXPERIMETION

2.1 Synthesis of Compound 9-(8-bromooctyl)-9H-carbazole

Next,5 mL toluene, 0.5 mL NaOH aqueous solution with a mass fraction of 50% and triethyl benzyl ammonium chloride (0.046 g, 0.2016 mmol) as alkylation catalyst were added to a 25 mL single-neck flask and stirred at room temperature for 30 mins. Carbazole (0.7 g, 4.2 mmol) was added to the mixture, and the mixture was stirred at 50 °C for 1 hour to evenly disperse it to improve the reaction yield. 1,8-Dibromooctane (0.8 mL) was slowly added to the reaction solution and reacted at 50 °C for 12 hours. After the reaction, the mixture was extracted with methylene chloride, combined with the organic phase, washed with deionized water three times and saturated salt water one time, and then dried with anhydrous magnesium sulfate. The excess organic solvent was removed by a rotary evaporator, the solid product was separated and purified by a silica gel column (the eluent was petroleum ether: dichloromethane = 20:1), and a colourless oily liquid compound (1.36 g, 91%) was obtained. ^{1}H NMR

(600 MHz, $CDCl_3$) δ 8.08 (d, 2H), 7.45 (t, 2H), 7.37 (d, 2H), 7.22 (t, 2H), 4.26 (t, 2H), 3.34 (t, 2H), 1.84 (m, 2H), 1.78 (m, 2H), and 1.28 (m, 8H).

2.2 Synthesis of the monomer 9-(8(9H-carbazol-9-yloctyl)-2,7-dibromo-9H-carbazole

2,7-Dibromo-9H-carbazole (292.5 mg, 0.9 mmol) and NaH (29 mg, 1.2 mmol) were added to THF (4 mL) and stirred at room temperature for 1 hour. 9-(8-bromooctyl)-9H-carbazole (214.9 mg, 0.6 mmol) was slowly added to the mixture and stirred at room temperature for 48 h. After the reaction, the solvent was removed by rotary evaporation, deionized water (15 mL) was added to the residual solid, and then dichloromethane was utilized for extraction (3×30 mL). All organic phases were combined and dried overnight with anhydrous Mg_2SO_4; the solvent was removed by rotating evaporation; and the white floc (0.296 g, 82%) was obtained by recrystallization with dimethylsulfone (DMSO). ^{1}H NMR (600 MHz, $CDCl_3$) δ 8.08 (d, 2H), 7.87 (d, 2H), 7.50 (s, 2H), 7.45 (t, 2H), 7.38 (d, 2H), 7.33 (d, 2H), 7.22 (t, 2H), 4.28 (t, 2H), 4.14 (t, 2H), 1.84 (m, 2H), 1.77 (m, 2H), 1.36 (m, 8H). ^{13}C NMR ($CDCl_3$, ppm): 141.35, 140.43, 125.56, 122.83, 122.55, 121.46, 121.29, 120.31, 119.70, 118.72, 111.99, 108.64, 77.27, 77.02, 76.76, 43.21, 43.00, 41.04, 29.14, 29.02, 28.81, 28.57, 27.13, and 26.94.

2.3 Synthesis of polymer PCZBDTCZ

The monomers 9-(8(9H-carbazol-9-yloctyl)-2,7-dibromo-9H-carbazole (60.3 mg, 0.1 mmol) and 4,8-bis(5-(2-ethylhexyl) thiophen-2-yl)benzo[1,2-b:4,5-b']dithiophene-2,6-diyl)bis(trimethylstannane) (BDT75) (90.5 mg, 0.1 mmol) were added to a 25 mL three-necked flask. Next, a mixed solvent of anhydrous toluene (4 mL) and anhydrous DMF (0.4 mL) was added. After nitrogen blowing deoxygenation of the solution, $Pd_2(dba)_3$ (4 mg) and $P(o\text{-}tol)_3$ (10 mg) were quickly added. The reflux device and the three-way device were quickly installed, and nitrogen was repeatedly filled with vacuum three times. At 110 °C for 40 hours, the colour of the mixture changed from yellow–green to orange. After cooling to room temperature, the mixture was dropped into a methanol solution and stirred by a magnetron for precipitation treatment. The precipitates were collected by filtration and extracted with acetone and n-hexane for 12 hours. Next, the solid was dissolved with chloroform and dropped into methanol again for precipitation. The precipitate was collected by filtration and dried under vacuum at 30 °C to obtain polymer PCZBDTCZ (88.2 mg, Mn=13.35 kDa, Mw=27.50 kDa, and PDI=2.06).

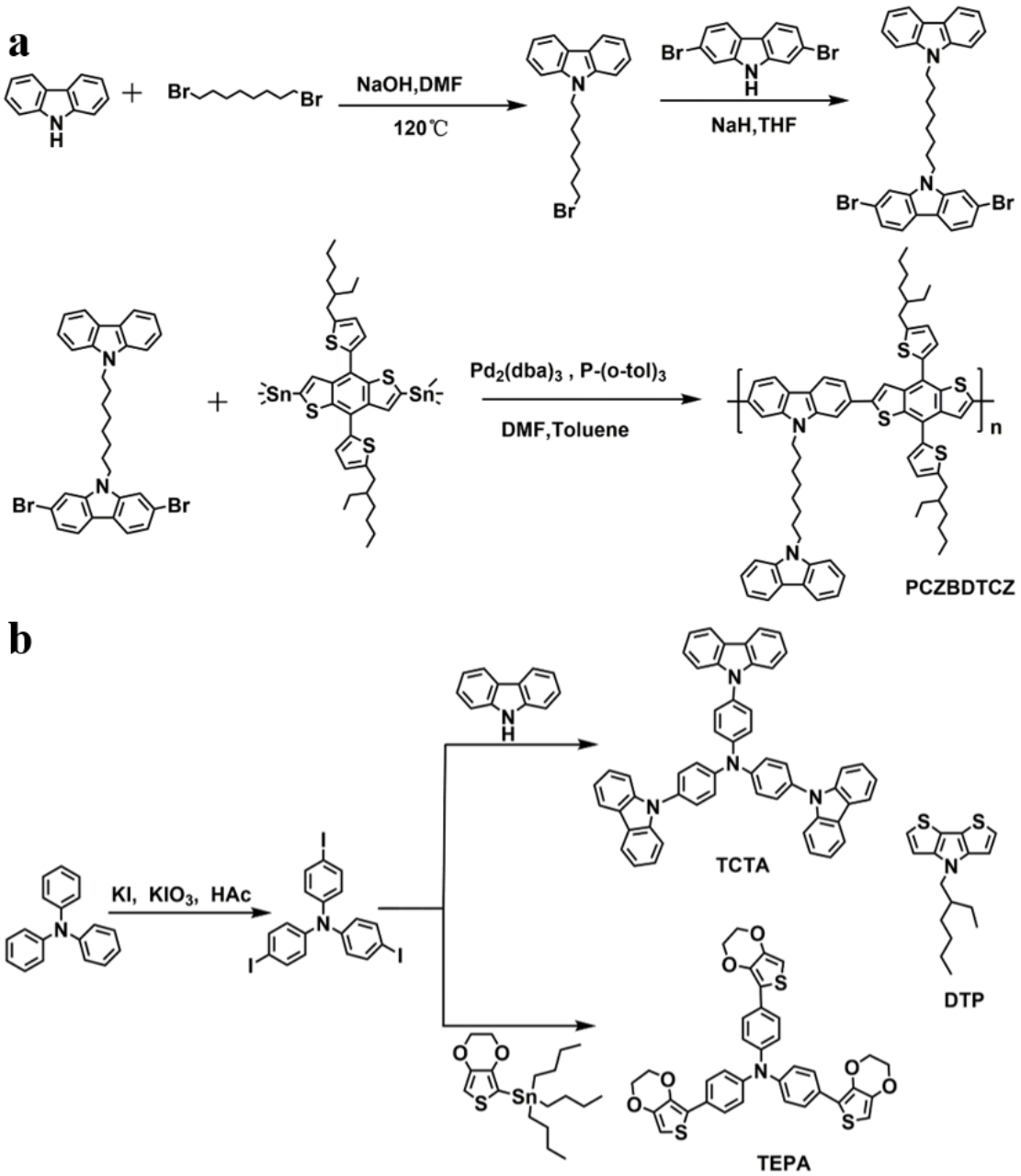

Figure 1. (a) Synthesis routes of polymer PCZBDTCZ, (b) Synthesis routes of cross-linking agents TCTA and TEPA.

2.4 Synthesis of tris(4-iodotriphenyl) amine

Five grams of triphenylamine and 7.5 g of KI were placed in a 25 mL three-way flask, and 70 mL of glacial acetic acid was added and stirred until dissolved. A total of 4.8 g of KIO_3 was added three times and reacted at 120 °C for 4 hours. After the reaction ended, the mixed liquid was cooled to room temperature and poured into a beaker, and a small amount of deionized water was added to precipitate a solid. $NaHSO_4$ was added to the beaker for stirring and filtration. The saturated $NaHCO_3$ solution was continuously washed until no bubbles were generated, and the powdery and white solids were collected and dried (4.62 g, 36%). ^{1}H NMR (600 MHz, $CDCl_3$) δ 7.54 (d, 6H), and 6.83 (d, 6H).

2.5 Synthesis of crosslinking agent tris(4-(9H-carbazole-9-yl) phenyl) amine (TCTA)

Tris(4-iodotriphenyl) amine (2.37 g, 3.8 mmol), carbazole (2.25 g, 13.43 mmol), CuI (0.22 g), potassium carbonate (2 g) and 1,10-phenanthroline (0.5 g) were added to a 50 mL three-way flask. N,N-dimethylacetamide solvent (20 mL) was added to the mixture in a nitrogen atmosphere at 166 °C with reflux for 24 hours. After the reaction, the mixture was extracted with ethyl acetate, combined with the organic phase, washed with water three times, and then washed with saturated salt water. Anhydrous magnesium sulfate was added and dried overnight. The product was purified by silica gel column (the eluent was petroleum ether:ethyl acetate = 2:1). The final product was a yellowish brown solid (0.85 g, 30%). ^{1}H NMR (600 MHz, $CDCl_3$) δ 8.17 (d, 6H), 7.60-7.42 (m, 24H), and 7.31 (t, 6H).

2.6 Synthesis of crosslinking agent tris (4-(2,3-dihydrothieno[3,4-b] dioxin-5-yl) phenyl) amine (TEPA)

Tris (4-iodotriphenyl) amine (20.77 mg, 0.033 mmol) and tributyl (2,3-dihydrothieno[3,4-b] [1,4] dioxin-5-yl) stannane (43.2 mg, 0.11 mmol) were added to a 25 mL, three-mouth flask. Next, 2 mL anhydrous toluene and 0.2 mL anhydrous DMF were added, and the device was deoxygenated. $Pd_2(dba)_3$ (4 mg) and $P(o\text{-}tol)_3$ (10 mg) were quickly added, filled with nitrogen in a vacuum three times, and refluxed at 120 °C for 24 hours. It was observed that the mixture changed from purplish red to yellow brown; that is, the catalyst successfully worked. After the reaction was cooled to room temperature, dichloromethane was selected to extract the mixture three times, and the organic phase was combined and washed with deionized water and then washed with saturated salt water. Afterward, anhydrous magnesium sulfate was added to the organic phase and dried overnight. The excess solvent was removed with a rotary evaporator, and the product was purified by silica gel column (the eluent was petroleum ether: dichloromethane =7:3). The final product was a white–green solid (25.3 mg, 38%). ^{1}H NMR (600 MHz, $CDCl_3$) δ 7.58 (d, 6H), 7.10 (d, 6H), 6.26 (s, 3H), and 4.30–4.25 (m, 12H).

2.7 Electrode preparation

The crosslinked polymer electrode was prepared by electropolymerization. First, ITO conductive glass was ultrasonically cleaned with ethanol, isopropyl alcohol and acetone for 15 minutes, and then N_2 was employed to blow dry the solvent on the ITO surface for subsequent use to complete the pretreatment of ITO. The configuration of the electropolymerization electrolyte was to add 3.87 g tetrabutylhexafluorophosphoric amine (TBAPF6) to 100 mL dichloromethane to obtain a concentration of 0.1 M TBAPF6-CH_2Cl_2 solution, and then 10 mg polymer PCZBDTCZ was added to the solution with a concentration of 0.1 mg mL^{-1} as the standard. The solution was stirred until dissolved, and N_2 was poured into the solution. During the process of electropolymerization, pretreated ITO served as the working electrode; platinum wire was selected as the opposite electrode; a 10 mM Ag/Ag^{+} electrode served as the reference electrode; and the volume of the electropolymerization electrolyte was 30 mL. The polymer PPCZBDTCZ film was prepared by cyclic voltammetry, setting the voltage parameter range to 0-0.95 V, setting the scanning rate to 50 mV/s, and setting the cycle number to 30 times. Next, the film deposited on ITO was washed with acetonitrile and naturally dried. The PPCZBDTCZ-TCTA

and PPCZBDTCZ-TEPA thin films were obtained by adding 1.5 mg crosslinking agents TCTA and TEPA to 30 mL electrolyte and evenly stirring. The polymer film PPCZBDTCZ-DTP was fabricated by a constant voltage method by adding 2 mg crosslinking agent DTP46 to 30 mL electrolyte and evenly stirring, setting the polymerization voltage to 0.95 V and the polymerization time to 500 s. After electropolymerization, the voltage was changed to 0 V, and the polymerization time was set to 60 s to obtain the neutral state of the film. The electrode was cleaned with acetonitrile and dried in a natural environment. We added 3 mg of crosslinking agent DTP46 and 1 mg of crosslinking agent TEPA to 30 mL electrolyte solution and evenly stirred it to obtain mixed crosslinking agent D3P1. The polymer electrode PPCZBDTCZ-D3P1-1 was obtained by using the same constant voltage method as that employed to prepare PPCZBDTCZ-DTP. PPCZBDTCZ-D3P1-2 and PPCZBDTCZ-D3P1-3 were prepared by using the same cyclic voltammetry method chosen to prepare PPCZBDTCZ. The difference was that the voltage range of the PPCZBDTCZ-D3P1-3 electrode was changed to -0.2-0.95 V. Table 1 shows the preparation conditions of the abovementioned polymer electrodes.

Table 1. Preparation conditions of the polymer electrode.

Polymer electrode	Electropolymerization method	Voltage parameter
PPCZBDTCZ	Cyclic voltammetry	0-0.95 V
PPCZBDTCZ-TCTA	Cyclic voltammetry	0-0.95 V
PPCZBDTCZ-TEPA	Cyclic voltammetry	0-0.95 V
PPCZBDTCZ-DTP	Constant Voltage	0.95 V
PPCZBDTCZ D3P1-1	Constant Voltage	0.95 V
PPCZBDTCZ D3P1-3	Cyclic voltammetry	-0.2-0.95 V

3. RESULTS AND DISCUSSION

3.1 Synthesis of polymer and cross-linking agents

The synthesis route of the polymer PCZBDTCZ is shown in Figure 1(a). The polymer PCZBDTCZ was successfully synthesized through a two-step substitution reaction and a one-step Stille cross-coupling reaction by using carbazole and 1,8-dibromooctane as starting materials. Many studies have investigated the copolymerization of two different types of electrochemically active groups, such as pyrrole and thiophene derivatives, thiophene and carbazole, pyrrole and indole [31-33]. Here, we designed three different cross-linking agents for polymerization with the previously prepared polymer PCZBDTCZ. The cross-linking agent DTP with a plane-rigid conjugate structure was directly purchased, while TCTA and TEPA with a large nonplane-rigid conjugate system were synthesized. The structure and synthesis routes of TCTA and TEPA are shown in Figure 1(b). Both TCTA and TEPA are synthesized from tris(4-iodophenyl) amine. Among them, TCTA was synthesized from tris(4-iodophenyl) amine and carbazole through substitution reaction, and TEPA was synthesized by Stille cross-coupling reaction. Their structures were also confirmed by ^{1}H NMR.

3.2 Electropolymerization process and thin film morphology of crosslinked polymers

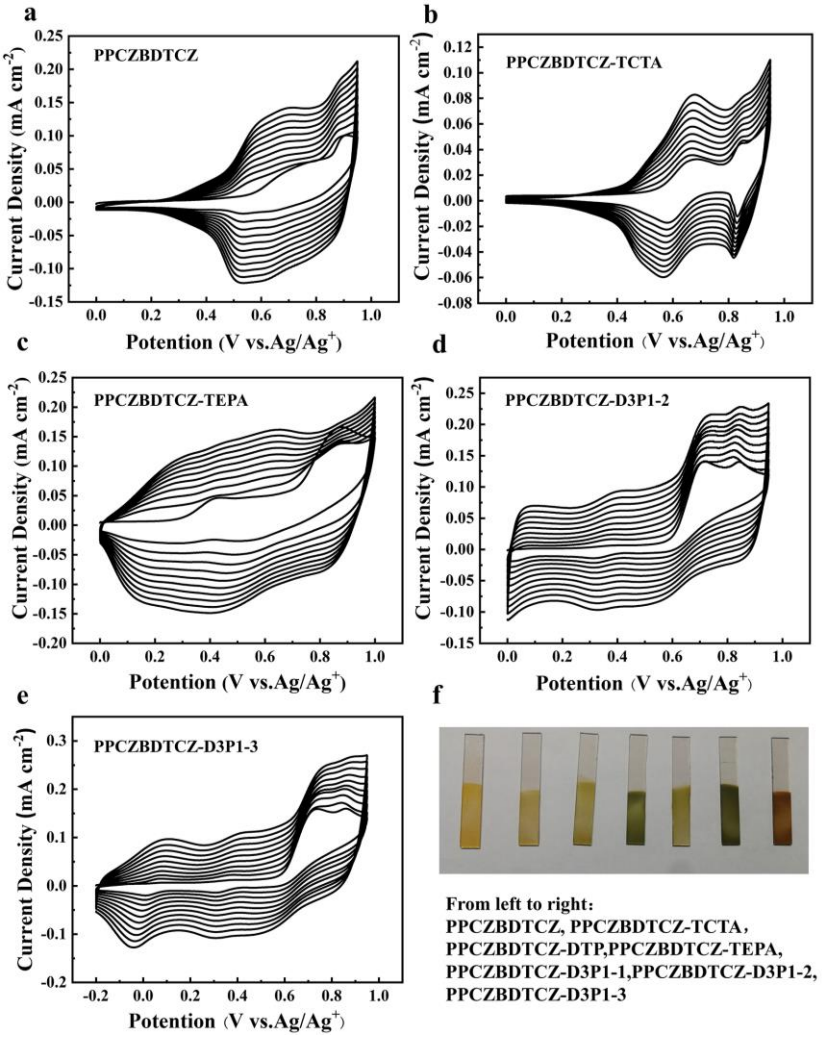

Figure 2. Electropolymerization CV curves of cross-linked polymers (a) PPCZBDTCZ, (b) PPCZBDTCZ-TCTA, (c) PPCZBDTCZ-TEPA, (d) PPCZBDTCZ-D3P1-2, (e) PPCZBDTCZ-D3P1- 3, (f) Photograph of cross-linked polymer film electrode.

Figure 2a shows the cyclic voltammetry curve of pure polymer PCZBDTCZ during the process of electropolymerization. Carbazole groups were introduced to the side chain of the polymers to be electrically polymerized under the action of an applied voltage; thus, we successfully deposited on the surface of the working electrode. During the second cycle curve, a new oxidation peak appeared near 0.58 V, which can be attributed to the oxidation peak of the dimer formed by the electropolymerization of side-chain carbazole groups. The electropolymerization curves of polymer PCBDTCZ mixed with different crosslinkers suggested that the cyclic voltammogram curves of polymer with crosslinkers significantly changed, demonstrating that the types of crosslinker had a significant impact on the polymerization process (Figure 2b-e). After the addition of the cross-linking agent TCTA, the redox peak became sharper during the electropolymerization of PCZBDTCZ, and the electrochemical activity range of TCTA surpassed 1 V. With the addition of the crosslinking agents TEPA and D3P1, the redox interval of the materials was widened, which represented improvement in the electrochemical activity. In addition, during the process of electropolymerization, the current density of the CV curve regularly

increased with the increasing number of scanning cycles, and the colour of the polymer films also changed with the applied voltage[34]. Simultaneously, a layer of polymer film can be gradually observed on the electrode surface, indicating that the polymer film evenly grew on the ITO surface and that the redox properties were constantly improved. As shown in Figure 2f, seven polymer films obtained by electropolymerization had obvious colour differences in appearance, indicating that the crosslinker had a great influence on the intramolecular charge transfer and conjugation length.

3.3 Analysis of electrochromic properties

By measuring the optical changes of cross-linked polymer films under different applied voltages, their electrochromic properties were investigated. The electrochemical test was carried out with $LiClO_4$/PC solution as the electrolyte in a three-electrode system. The cuvette served as an electrolytic cell; the reference electrode was a silver wire; and the counter electrode was a platinum wire. The UV–vis absorption spectra of crosslinked polymers under different applied voltages are illustrated in Figure 3a-f, and the internal illustrations are digital photographs of the films in different colour states. With the exception of the poor spectral electrochemical properties of the polymer PPCZBDTCZ-D3P1-2, it will not be discussed further.

As shown in the UV-vis absorption spectrum in Figure 3a, the maximum absorption value of PPCZBDTCZ was 480 nm, the UV absorption peak gradually decreased with increasing applied voltage, and the UV absorption value gradually increased at 700 nm. When a voltage of 0.7 V was applied, the colour of the polymer film started to change, gradually changing from orange yellow to light blue. The maximum absorption wavelengths of the other five polymers in the original state were 483 nm, 472 nm, 462 nm, 467 nm, and 470 nm. The colour change of the PPCZBDTCZ-TCTA film prepared by electric polymerization of the cross-linking agent based on TCTA was similar to that of the pure polymer film PPCZBDTCZ, and the initial colour change voltage was 0.7 V (Fig. 3b). The film PPCZBDTCZ-TEPA fabricated by the same cyclic voltammetry as the above two films also showed different colour changes from yellow green to light blue and then to dark-blue–grey (Fig. 3d). However, due to the addition of the DTP cross-linking agent, the PPCZBDTCZ-DTP film prepared by constant pressure polymerization exhibited more diverse colour changes. When a voltage of 0.3 V was applied, it experienced a series of rich and distinct colour changes ranging from orange–red to pale yellow, from pale yellow to green and then from green to blue (Fig. 3c). In addition, the film colour changes of PPCZBDTCZ-D3P1-1 and PPCZBDTCZ-D3P1-3 obtained by different polymerization methods with the same cross-linking agent were also obviously different. PPCZBDTCZ-D3P1-1 changed from yellow to light blue and then to blue (Fig. 3e), while PPCZBDTCZ-D3P1-3 changed from orange–red to emerald green to blue (Fig. 3f), exhibiting that the different polymerization methods had an important influence on the content of the crosslinking agent in the final polymers. The content of the crosslinking agent DTP in PPCZBDTCZ-D3P1-1 films obtained by constant voltage polymerization was less than that of PPCZBDTCZ-D3P1-3 films polymerized by cyclic voltammetry. Moreover, under the synergistic effect of DTP and TEPA, the initial discolouration voltage of the electropolymerized polymer film was as low as 0.1 V.

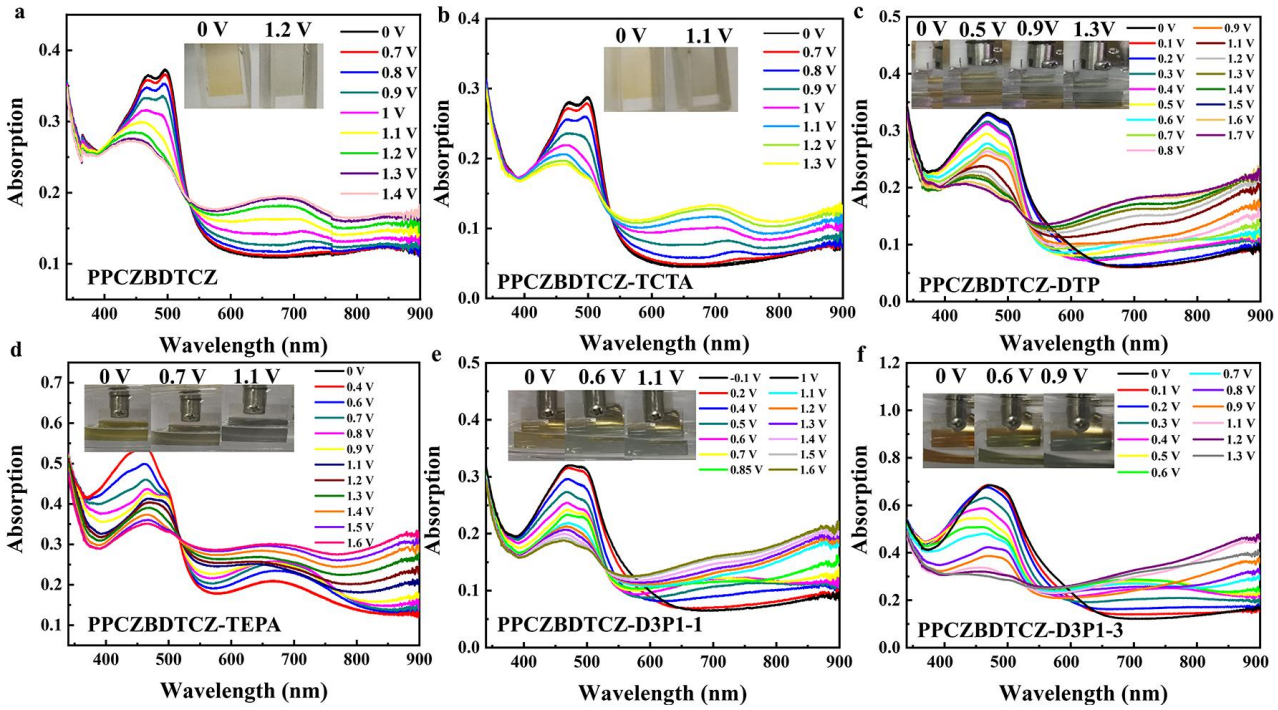

Figure 3. UV-vis absorption spectrum of crosslinked polymers (a) PPCZBDTCZ, (b) PPCZBDTCZ-TCTA, (c) PPCZBDTCZ-DTP, (d) PPCZBDTCZ-TEPA, (e) PPCZBDTCZ-D3P1-1, (f) PPCZBDTCZ-D3P1-3 under different applied voltages (the upper and lower insets show the film colour at the corresponding voltage).

Figure 4a-f shows the light absorption conversion curves of the six films, with the exception of PPCZBDTCZ-D3P1-2, at their respective maximum absorption wavelengths. The response time of an electrode material refers to the time it takes for the electrode material to change from a colored state or a bleached state to another state, which is used to describe the speed of the electrode material's discoloration rate, calculated as the time when the transmittance changes by 90% [35]. The response time depends mainly on the ability of the electrolyte to conduct ions and the ease of diffusion of these counterion species on the electrochromic electrode [36]. As shown in Figure 4a-f, the coloring times of the six films were 1.1s, 1.9s, 1.2s, 2.7s, 0.9s and 3.2s, and the bleaching times were 0.4s, 0.6s, 4.4s, 4.2s, 1.3s and 4.6s respectively. Contrast with previously reported research work, the response times of the six polymer materials prepared in this work are more excellent, for instance, V_2O_5 xerogel film (5.0 s for the coloring time and 6.2 s for the bleaching time), Fe(0.41)V_2O_5 xerogel film (12.6 s for the coloring time and 7.0 s for the bleaching time)[37], and cyclometalated platinum phenylacetylide [(L)Pt(C[triple bond, length as m-dash]C–ph)]{L=4-[p-(diphenylamino)phenyl]-6-phenyl-2,2′-bipyridine}(6.5 s for the coloring time and 9.5 s for the bleaching time)[38].

Optical contrast (ΔT) refers to the difference between the light transmittance (T_c) in the colored state and the light transmittance (T_b) in the faded state of the electrochromic film material at a specific wavelength, generally expressed as a percentage. It is a standard for measuring the strength of the color change of electrochromic materials, which can be calculated by formula (1).

$$\Delta T=|T_b-T_c| \quad (1)$$

The optical contrasts of the six polymer materials were 11.82% at 480nm, 10.50% at 483nm, 11.94%

at 472nm, 12.37% at 462nm, 14.57% at 467nm and 17.36% at 470nm. It can be found that the PPCZBDTCZ-D3P1-3 had the largest value (17.63%), which was superior to the optical contrast of the two ladder-like donor-acceptor (D-A) polymer electrode materials, PI-BT(4.05% at 491.5nm) and PI-DPP(6% at 599nm), and PDTCZ-1(10.3% at 660nm) previously reported [39,40].

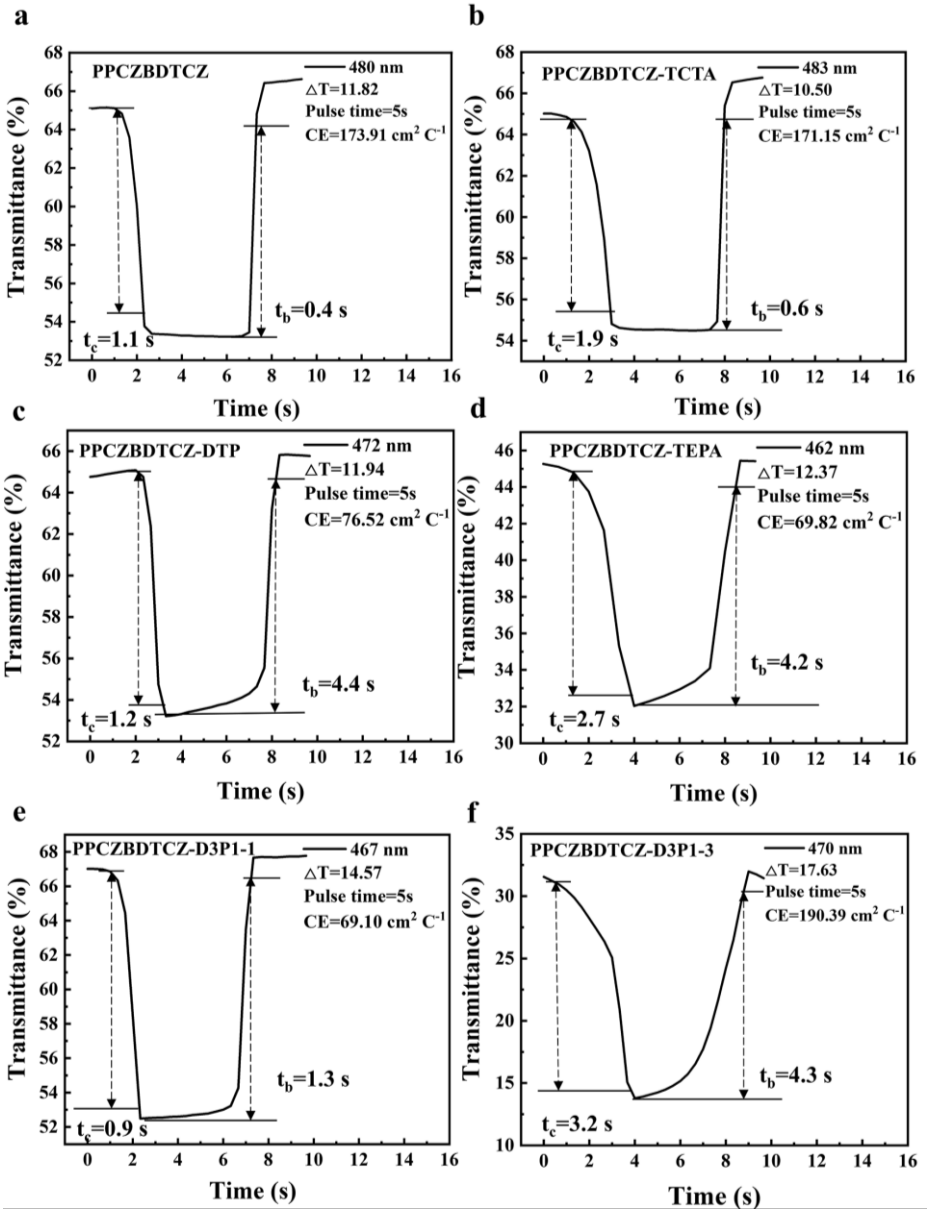

Figure 4. The absorption conversion curve of cross-linked polymer (a) PPCZBDTCZ, (b) PPCZBDTCZ-TCTA, (c) PPCZBDTCZ-DTP, (d) PPCZBDTCZ-TEPA, (e) PPCZBDTCZ-D3P1-1, (f) PPCZBDTCZ-D3P-3 at a fixed wavelength.

The coloring efficiency (CE) is the ratio of the optical conversion density (ΔOD) during the redox process to the amount of charge injected per unit area of the electrode (Q_d), which is an inherent property of the electrode. The higher the CE of the electrochromic material, the higher the ion transfer efficiency can be achieved at a lower applied voltage, which indicates that the electrochromic material has better ion transport and charge transfer performance. The CE can be calculated by formula (2), where the unit of Q_d is C cm^{-2} and the unit of CE is cm^2 C^{-1}[41]. The ΔOD in formula (2) refers to the logarithm of the

ratio of the transmittance ratio of the colored state to the bleached state of the electrode material at a specific wavelength, which can be calculated according to formula (3) [42].

$$CE=\Delta OD/Q_d \quad (2)$$

$$\Delta OD=\log(T_b/T_c) \quad (3)$$

Among all polymer electrode materials obtained by electropolymerization, PPCZBDTCZ, PPCZBDTCZ-TCTA and PPCZBDTCZ-D3P1-3 exhibited significantly advanced colouring efficiency, which were 173.91 cm^2 C^{-1} at 480 nm(Fig. 4a), 171.15 cm^2 C^{-1} at 483 nm(Fig. 4b), and 190.39 cm^2 C^{-1} at 470 nm(Fig. 4f), respectively, and were superior to other electrode materials for electrochromic supercapacitors, such as poly(indole-6-carboxylic acid) vertical nanowire arrays (142 cm^2 C^{-1} at 490 nm)[43], zinc oxide (ZnO)/poly(3,4-ethylenedioxythiophene) (PEDOT) core/shell hybrid nanotube arrays (122.2 cm^2 C^{-1} at 520 nm)[44], PFETQ(157 cm^2 C^{-1} at 458nm), PFMTQ(130.4 cm^2 C^{-1} at 442 nm), and PFTQ(90.8 cm^2 C^{-1} at 590nm) [45], etc.

By comparing Figure 4e and 4f, we discovered that the polymer film prepared by cyclic voltammetry had excellent optical contrast and colouring efficiency, while the polymer film prepared by the constant voltage method had a faster response time. Due to the introduction of cross-linking agents with different structures, the response time and colouring efficiency of polymer films obtained by the same electropolymerization method differed. Compared with TCTA, the addition of the crosslinking agent TEPA lengthened the response time of the polymer film and reduced the colouring efficiency (Fig. 4b and 4d).

3.4 Surface morphology analysis

The connection between the electrode material obtained by electropolymerization and the substrate is stronger, and some researchers have found that the structure of carbazole-alkyl-carbazole (Cz-Cn-Cz) can be electropolymerized to obtain a cross-network structure [46], this unique structure can slow down the irreversible volume change of the electrode material due to the continuous insertion and extraction of electrolyte ions during electrochemical cycling[47], which is beneficial to improve the stability of the material. Scanning electron microscopy images of six crosslinked polymers are shown in Fig. 5, which clearly shows that all of them had many pore structures. Different electropolymerization methods can cause significant differences in the kinetics of the electropolymerization process and affect the morphology of the polymer films. The cyclic voltammetry electropolymerization tended to obtain smooth films, while the constant voltage polymerization allowed the polymer to remain in the doped state by applying a higher voltage, which was beneficial to the formation of a cross-linked grid structure in the polymer film. In addition, the different solubilities of polymers in the electrolyte solution were an important factor leading to the obvious difference in the surface morphologies of the films. The solubility of the polymer in the electrolyte solution was poor, and the film tended to nucleate during electropolymerization, producing a rough granular surface with a porous structure, while the solubility was moderate, and uneven grooves formed on the film surface. However, if the solubility was slightly better, the electropolymerization reaction was conducive to forming a uniform and flat film. As the solubility was too good, the polymer would not be able to deposit on the surface of the working electrode. Consequently, the six electropolymerized films exhibited different surface morphologies.

As shown in Fig. 5a, compared with other polymer films, the surface of the PPCZBDTCZ film without crosslinking agents was relatively flat. The surface of the PPCZBDTCZ-TCTA film was wrinkled rather than a large-area cross-linked lattice structure, since the carbazole groups in the cross-linking agent TCTA only form dimers (Fig. 5b). Fig. 5c shows that PPCZBDTCZ-DTP had a porous, dendritic, staggered grid structure, which was caused by the constant voltage polymerization method. As the cross-linking agent TEPA had strong rigidity and good conjugation, its three-prong, twisted structure loosened the cluster particles. Therefore, Fig. 5d shows that PPCZBDTCZ-TEPA had a visibly loose polymer packing morphology similar to an irregular sponge structure. Under the synergistic effect of the two cross-linking agents DTP and TEPA, the morphology of the PPCZBDTCZ-D3P1-1 film prepared by the constant voltage method was between a folded lattice and a cross-linked lattice (Fig. 5e), while the polymer PPCZBDTCZ-D3P1-3 film obtained by cyclic voltammetry electropolymerization had more holes, and the pore size was significantly reduced (Fig. 5f).

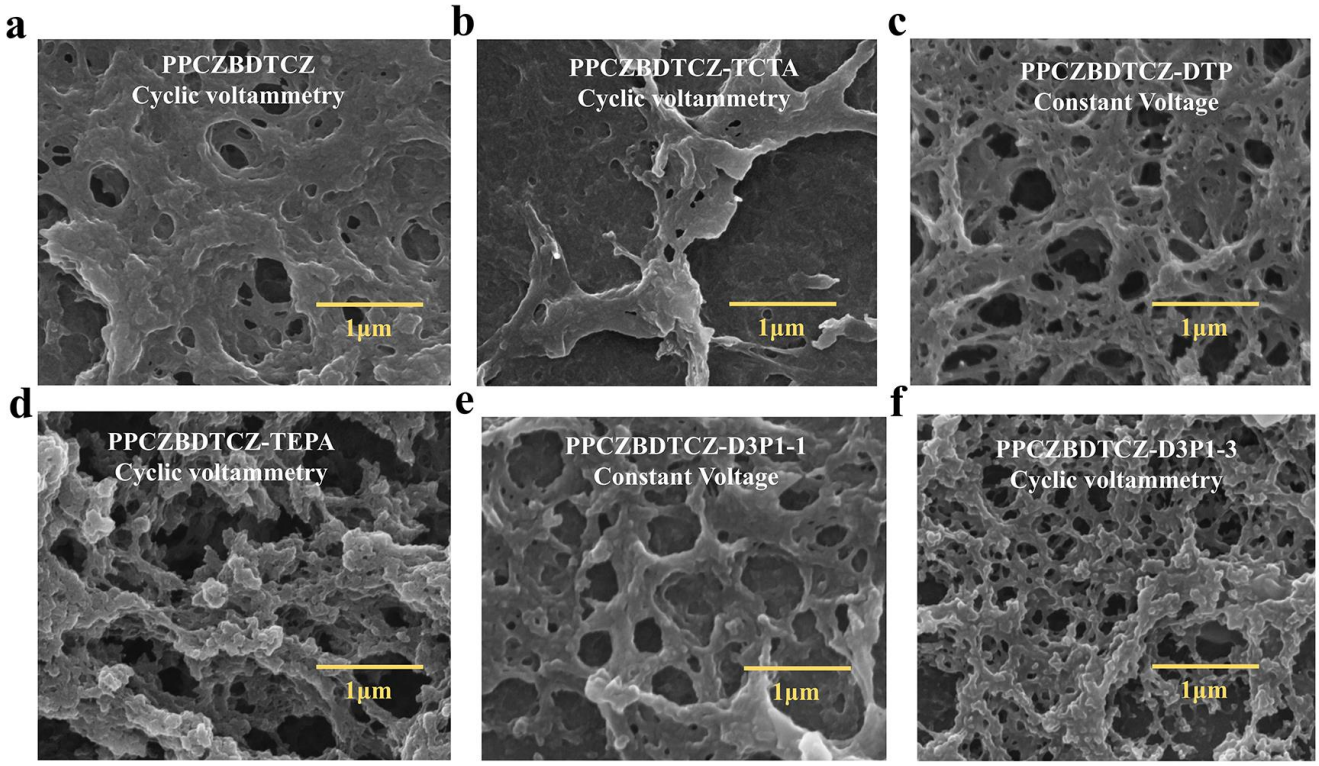

Figure 5. SEM picture of cross-linked polymer films (a) PPCZBDTCZ, (b) PPCZBDTCZ-TCTA, (c) PPCZBDTCZ-DTP, (d) PPCZBDTCZ-TEPA, (e) PPCZBDTCZ-D3P1-1, (f) PPCZBDTCZ-D3P1-3, the magnification was 80,000 times.

3.5 Electrochemical property analysis

To systematically investigate the electrochemical properties of cross-linked polymers, the cyclic voltammetry (CV), galvanostatic charge–discharge (GCD) and electrochemical impedance spectra (EIS) curves of thin film electrodes were measured using an electrochemical workstation [48]. The electrolyte solution selected for the test was 0.5 M $LiClO_4$/PC, with a platinum sheet electrode as the opposite

electrode and the Ag/Ag^+ electrode as the reference electrode. To ensure the accuracy of the experiment, all tests were carried out without water and oxygen.

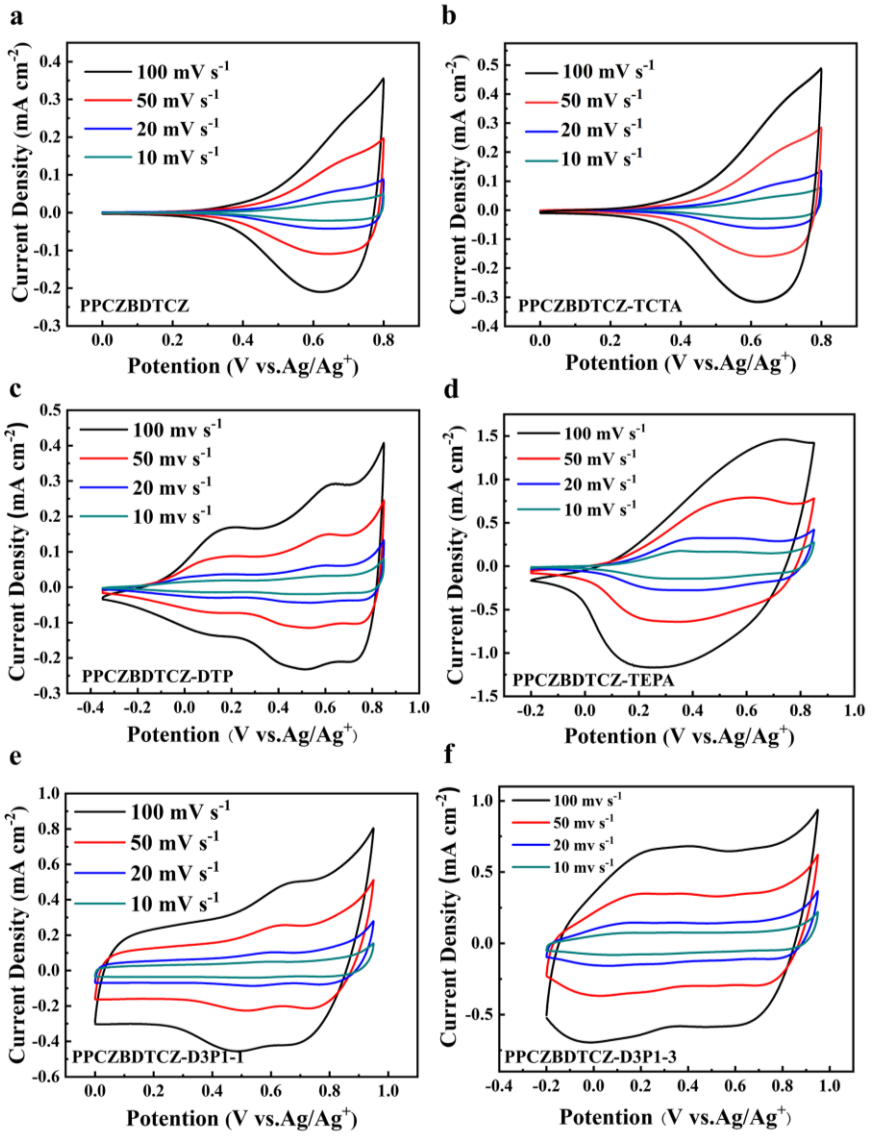

Figure 6. Cyclic voltammetry curves of cross-linked polymer electrodes at different scan rates (a) PPCZBDTCZ, (b) PPCZBDTCZ-TCTA, (c) PPCZBDTCZ-DTP, (d) PPCZBDTCZ-TEPA, (e) PPCZBDTCZ-D3P1-1, (f) PPCZBDTCZ-D3P1-3

The cyclic voltammetry curves showed that all the polymers exhibited significant pseudocapacitance properties (Fig. 6a-f). When the scanning rate increased from 10 mV S^{-1} to 100 mV S^{-1}, the CV curves of the six polymers did not significantly change, indicating that the materials had good rate capability [49]. A comparison of the CV curves of several polymer electrodes reveals higher peak current values of PPCZBDTCZ-TEPA (Fig. 6d) and PPCZBDTCZ-D3P1-3 (Fig. 6f), corresponding to larger areas of the CV curves and reflecting that both possessed higher capacitors. The redox peaks in the CV curve can be attributed to the conversion between different oxidation states of cross-linked polymers with various structures. The redox peak of the cross-linking agent TCTA appeared at a higher voltage of 1 V (vs. Ag/AgCl), so the CV curve of PPCZBDTCZ-TCTA did not change

significantly compared with that of PPCZBDTCZ (Fig. 6a-b) [50]. However, the redox peaks of the cross-linking agents DTP and TEPA appeared at -0.2 V (vs. Ag/Ag^{+}) and 0.6 V (vs. Ag-Wire), respectively (Fig. 6c-d), which made the voltage window of PPCZBDTCZ-DTP and PPCZBDTCZ-TEPA significantly higher than that of PPCZBDTCZ, benefiting the improvement of electrode material specific capacitance and device energy density. Therefore, PPCZBDTCZ-D3P1-1 and PPCZBDTCZ-D3P1-3 obtained by the synergistic action of DTP and TEPA not only improved the voltage window but also showed that the redox process was more reversible by comparing the integral area of the upper and lower parts of the CV curve (Fig. 6e-f). Furthermore, the shape of the CV curve of PPCZBDTCZ-D3P1-3 resembled a rectangle, implying that the PPCZBDTCZ-D3P1-3 electrode had a fast and reversible charge storage mechanism.

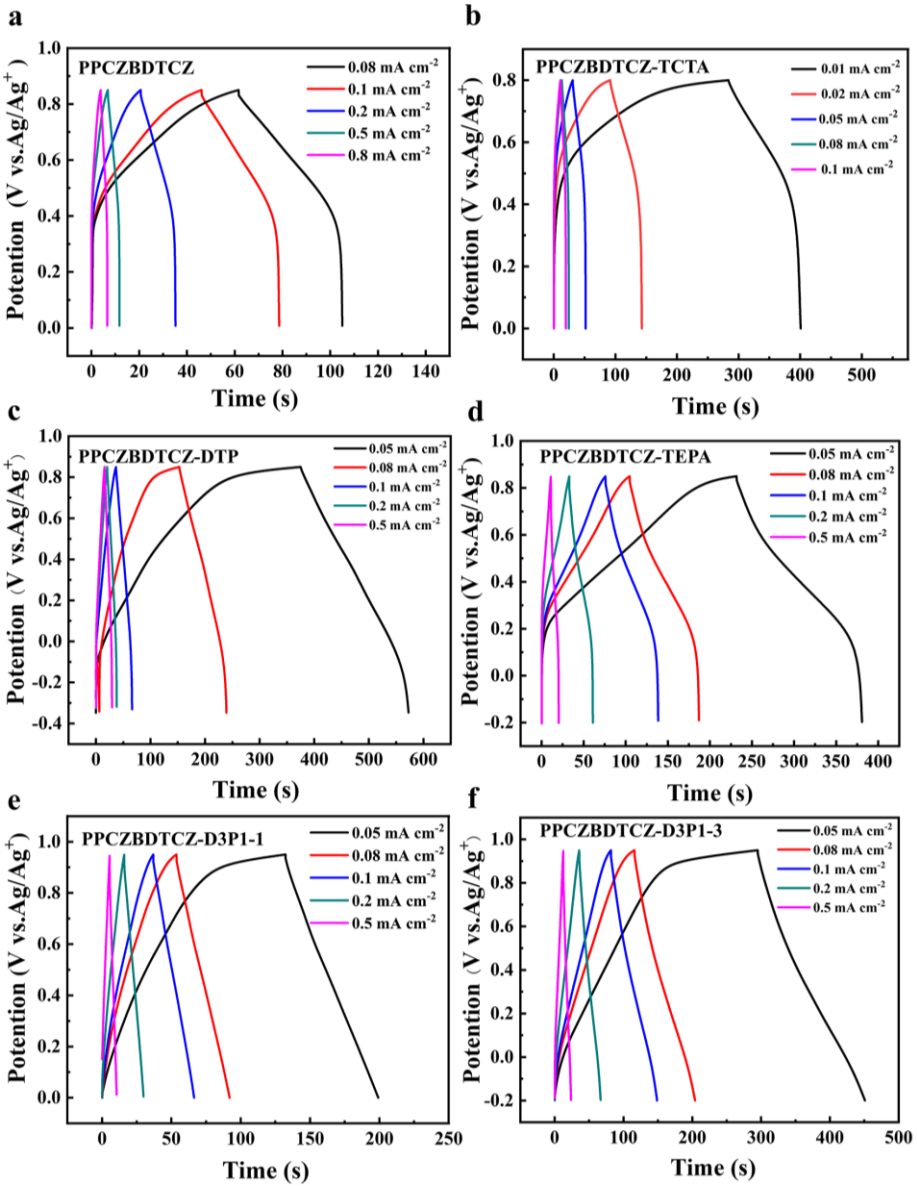

Figure 7. GCD curves at different currents density (a) PPCZBDTCZ, (b) PPCZBDTCZ-TCTA, (c) PPCZBDTCZ-DTP, (d) PPCZBDTCZ-TEPA, (e) PPCZBDTCZ-D3P1-1 and (f) PPCZBDTCZ-D3P1-3.

Figure 7a-f shows the charge–discharge curves of the six crosslinked polymer materials at different current densities tested by the galvanostatic charge–discharge method, which reflected obvious pseudocapacitance characteristics. The GCD curve showed that with decreasing current density, the charge and discharge time of the electrode materials were prolonged. By comparing the six sets of curves, the symmetry of the charge–discharge curves of the PCZBDTCZ and PCZBDTCZ-TEPA materials were significantly better than that of the other four curves. This highly symmetrical curve characteristic indicated that the two crosslinked polymer electrode materials had excellent electrochemical reversibility and coulombic efficiency [49]. Figure 7c, 7e and 7f shows that the symmetry of the GCD curves of the material was inferior to that of the other three figures, possibly attributed to the introduction of the crosslinking agent DTP, which enabled electrons to easily enter the material but hindered their extraction.

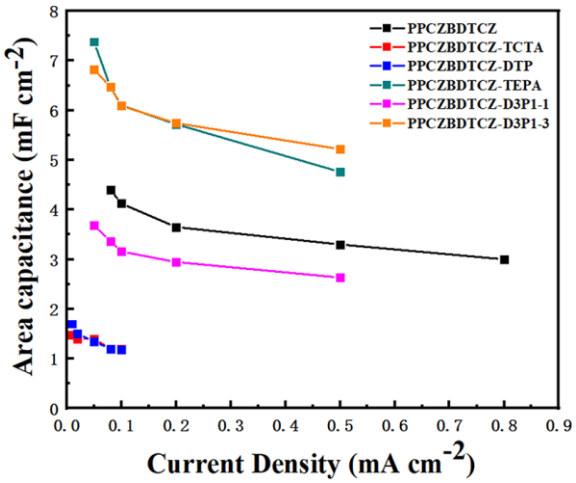

Figure 8. Area specific capacitance comparison of cross-linked polymer materials at different current densities.

According to the GCD curves, the specific capacitance (C_s, mF cm^{-2}) of the electrodes can be caculated according to the following formula (4) [51]:

$$C_s = I_A \cdot t/(A \cdot \Delta V) \quad (4)$$

where I_A is the current per unit area(mA), t is the discharge time of the material(s), A is the effective area of the electrode(cm^2), and ΔV is the voltage window of the electrode. A comparison of the area ratio capacitance of the six crosslinked polymer materials at different current densities is shown in Figure 8. At the same current density (0.08 mA cm^{-2}), the area ratio capacitances of PCZBDTCZ, PPCZBDTCZ-TCTA, PPCZBDTCZ-DTP, PPCZBDTCZ-TEPA, PPCZBDTCZ-D3P1-1 and PPCZBDTCZ-D3P1-3 were 4.4 mF cm^{-2}, 1.2 mF cm^{-2}, 1.25 mF cm^{-2}, 6.4 mF cm^{-2}, 3.3 mF cm^{-2} and 6.5 mF cm^{-2}, respectively. A comparison of the experimental results revealed that the addition of the crosslinking agent TEPA was beneficial to the increase in the area specific capacitance of the crosslinking polymer, while the addition of the crosslinking agents DTP and TCTA significantly reduced the area specific capacitance of the crosslinking polymer. Fortunately, the capacitance of the crosslinked polymer electrode PPCZBDTCZ-D3P1-3 only decayed 22% when the current density was improved by a factor of 10 (0.05-0.5 mA cm^{-2}), which was 10% higher than that of the pure PPCZBDTCZ film, showing that it possessed both superior area specific capacitance and a good rate property. It may be

mainly attributed to the dense and uniform pore structure on the surface of PPCZBDTCZ-D3P1-3, and this structure provides a larger contact area for electrolyte ions, so it demonstrated slightly better specific capacitance than other reported electrode materials. However, the area specific capacitance of polymers obtained in this work was moderate, there is still a certain gap in compared with the excellent performance of other researchers [52,53].

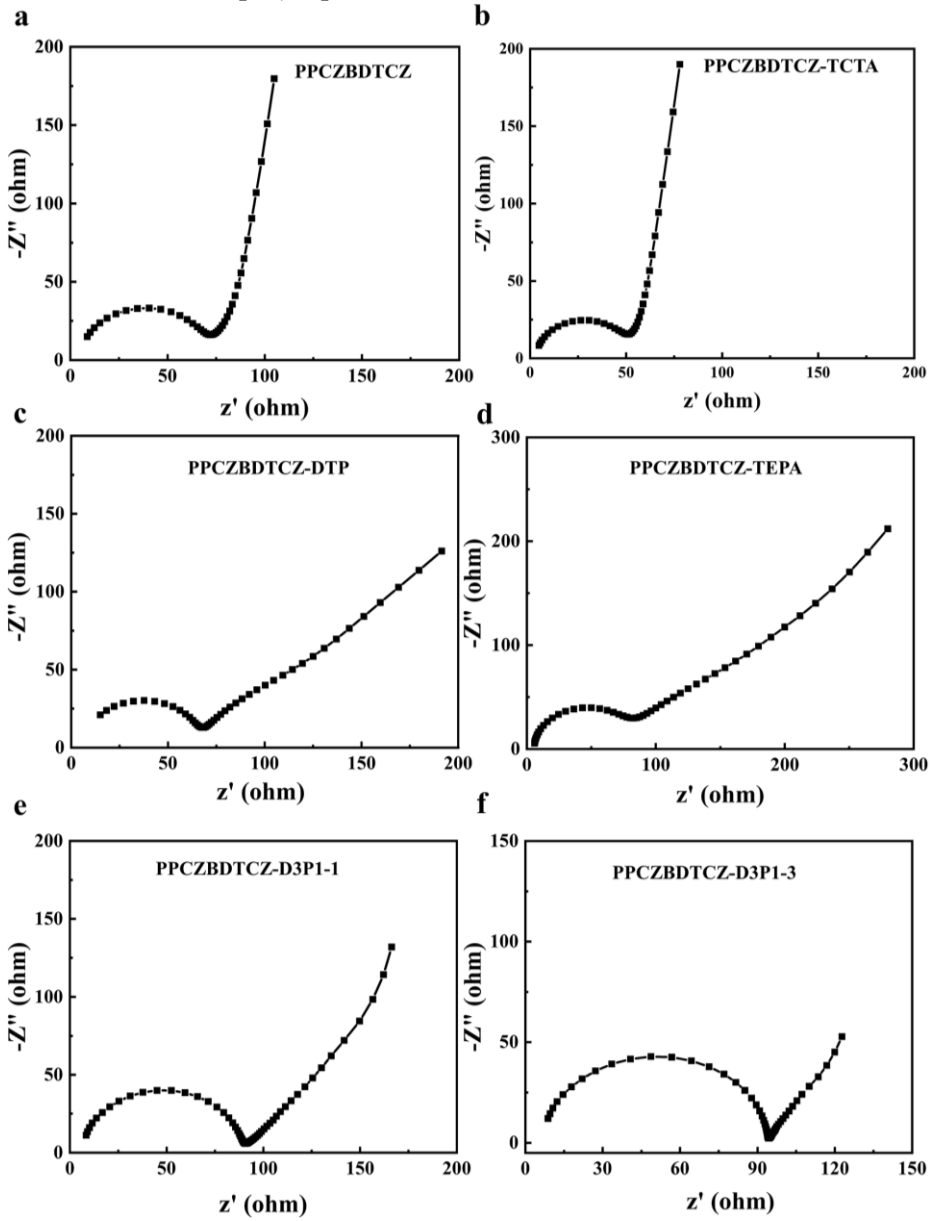

Figure 9. Nyquist curve of cross-linked polymers electrode (a) PPCZBDTCZ, (b) PPCZBDTCZ-TCTA, (c) PPCZBDTCZ-DTP, (d) PPCZBDTCZ-TEPA, (e) PPCZBDTCZ-D3P1-1, (f) PPCZBDTCZ-D3P1- 3.

Electrochemical impedance spectroscopy (EIS) testing has been considered as one of the most effective methods to characterize the conductivity and charge transport properties of electrode materials. The Nyquist diagram is generally composed of a semicircle in the high-frequency region and a straight line in the low-frequency region. The semicircle in the high-frequency region represents the charge transfer resistance (R_{ct}) between the electrode and the electrolyte, while the straight line in the low-frequency region reflects the diffusion resistance (R_0) of ions in the electrolyte and electrode. And

researchers have found that the diameter of the semicircle in the high-frequency region is inversely proportional to the conductivity, and the steeper the straight line in the low-frequency region, the more conducive to ion transport [54-56]. The EIS was performed to investigate the conductivity and ionic diffusion resistance of the six crosslinked polymers (Figure 9a-f). Zview software was selected to design equivalent circuit diagrams of the six crosslinked polymers. The calculated specific resistance values are shown in Table 2. The slopes of the straight lines in Fig. 9a and Fig. 9b were larger than those in the other four images, implying that PPCZBDTCZ and PPCZBDTCZC-TCTA had lower ion transport resistances than the other four polymers. The transfer resistances were 4.59 Ω and 3.08 Ω, respectively, which were consistent with the previous results. The inclinations of the straight line in Fig. 9c-f were smaller, meaning that the ion transport performance of the four polymers was lower, which may be because the prepared polymer films were relatively thick, which increases the distance of ion diffusion and affects the efficiency of ion diffusion. In addition, the diameters of the curves in Fig. 9d-f were also larger, indicating that the charge transfer performance of the materials were reduced. Among them, PPCZBDTCZC-D3P1-3 had the worst charge transfer ability, and the resistance value of PPCZBDTCZC-D3P1-3 in the fitting data in Table 2 was also the largest (85.86 Ω). In conclusion, the results illustrated that TCTA, a three-branched crosslinker with carbazole groups at the end, significantly reduced the charge transfer resistance and ion diffusion resistance of the PPCZBDTCZC-TCTA film. This finding may be mainly attributed to the notion that the carbazole groups with rigid twisted structures at the end of TCTA can only be dimerized. Thus, the polymer cannot be tightly packed and enhance the hole transport ability of the material, which also explain why PPCZBDTCZC-TCTA exhibited an ultrafast response time, corresponding to the previous results in Fig. 4b. In addition, the addition of a DTP crosslinking agent with a rigid conjugate plane significantly enhanced the conductivity of the material and reduced the charge transfer resistance of the crosslinking polymer (Fig. 9c).

Table 2. R_{ct} and R_0 comparison of cross-linked polymers simulated by Zview software.

Polymer	Charge-transfer resistance $R_{ct}(\Omega)$	Ion diffusion resistance $R_0(\Omega)$
PPCZBDTCZ	60.33	4.59
PPCZBDTCZ-TCTA	45.00	3.08
PPCZBDTCZ-DTP	55.60	5.04
PPCZBDTCZ-TEPA	67.77	5.46
PPCZBDTCZ-D3P1-1	81.85	6.66
PPCZBDTCZ-D3P1-3	85.86	7.13

Cycling stability is one of the important parameters to measure the electrochemical performance of electrode materials for supercapacitors [57]. The cyclic stability of the materials can be obtained by observing the CV curves of the six crosslinked polymers at a scanning rate of 100 mV s^{-1} (Figure 10a-f). A comparison of the integral area of the CV curves reveals that the capacitance of the polymer materials sharply attenuated in the first 100 cycles, but the trend of capacitance attenuation gradually decreased with the increasing number of cycles. The capacitance retention rates of the six polymers after 300 cycles were 71%, 45%, 59%, 84%, 66% and 73%, respectively. Since the TCTA cross-linking agent

can only form dimers in the polymerization reaction and cannot effectively avoid volume changes during electrochemical cycling, PPCZBDTCZ-TCTA had the worst cycling stability and could only experience 300 cycles (Fig. 10b). Benefiting from the synergistic effect of DTP and TEPA, PPCZBDTCZ-D3P1-1 and PPCZBDTCZ-D3P1-3 also showed good cycling performance, with the capacitance retention rate of 47% and 54% after 1000 cycles (Fig. 10e and 10f).

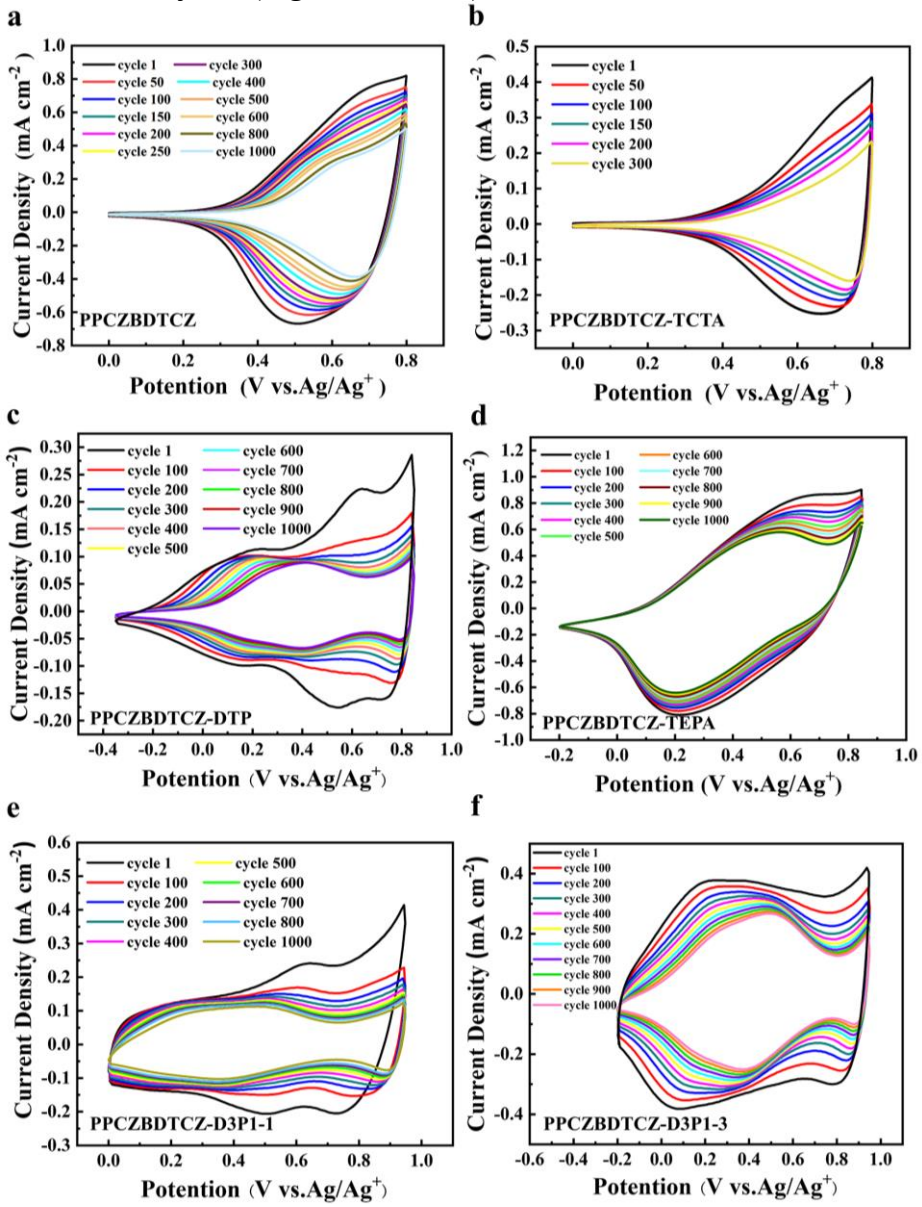

Figure 10. Cyclic voltammograms of cross-linked polymers (a) PPCZBDTCZ, (b) PPCZBDTCZ-TCTA, (c) PPCZBDTCZ-DTP, (d) PPCZBDTCZ-TEPA, (e) PPCZBDTCZ-D3P1-1, (f) PPCZBDTCZ-D3P1-3, scan rate 100 mV s^{-1}.

Observing Fig.9a and 9c, it can be found that PPCZBDTCA-DTP and PPCZBDTCA-DTP can also undergo 1000 CV cycles, but the capacitance retention rates of them were not ideal. Among the six polymer films, it is noteworthy that PPCZBDTCZ-TEPA had the best cyclic stability with a capacitance retention of 67% after 1000 cycles (Fig. 10d). As the EDOT group at the end of the crosslinking agent TEPA was easily polymerized and had good electrochemical activity, it was easy to form a large area of

crosslinked lattice structure, thus avoiding the reduction in the mechanical stability of the electrode material to a large extent. However, the cycling stability of the materials prepared in this work is very mediocre compared to the excellent cycling performance of other previously reported electrode materials for supercapacitors [58-60].

4. CONCLUSIONS

We synthesized the polymer PCBDTCZ with side chains modified by carbazole groups, which can be electropolymerized into the crosslinked polymer film. Furthermore, by introducing different crosslinking agents, a series of crosslinked polymers that show quite different film morphologies and electrochemical properties, were prepared. As the cross-linking agent TCTA had poor electrochemical activity, the carbazole groups at its end only form a dimer when electropolymerization occurs, and hence, large cross-networking lattice structures cannot be formed, leading to inferior electrochemical properties and cyclic stability. The polymer film with the three-branched cross-linking agent TEPA, which grafted EDOT groups with better electrochemical activity at the end, was more conducive to forming large-area, cross-networking lattice structures, contributing to improved capacitance and cyclic stability. Due to the synergistic effect of the mixed cross-linking agent D3P1, the redox reaction of PCBDTCZ-D3P1-3 prepared by cyclic voltammetry was more reversible, showing the best colouring efficiency (190.39 cm^2 C^{-1}) and the maximum area ratio capacitance (6.5 mF cm^{-2}) was superior to other crosslinked polymers, providing a new idea for the design of conjugated polymer-based electrode materials for smart supercapacitors.

ACKNOWLEDGMENTS
This research was supported by the National Natural Science Foundation of China (21374016 and 21304018), the Jiangsu Provincial Natural Science Foundation of China (BK20130619 and BK20130617). Ying Sun appreciates the support from “Southeast University Zhishan Young Scholar Program” (2242021R41090).

References

1. A. Berrueta, I. Ursúa, S. Martín, A. Eftekhari and P. Sanchis, *IEEE Access*., 7(2019)50869.
2. Z. Chen, J. Chen, F. Bu, P. Agboola, I. Shakir and Y. Xu. *ACS Nano*., 12(2018)12879.
3. G. Q. Wu, X.Y. Yang, J. H. Li, N. Sheng, C. Y. Hou, Y. G. Li and H. Z. Wang, *Chinese J. Polym. Sci*., 38(2020)531.
4. W.W. Kang, Y. Sun, B. Xu, J. Li, X. Kong, D.F. Huang, X. Q. Zhang, H. Yang and B. P. Lin, *Electrochim. Acta*., 323(2019)134819.
5. C. Largeot, C. Portet, J. Chmiola, P. Taberna, Y. Gogotsi and P. Simon, *J. Am. Chem. Soc.*, 130(2008)2730.
6. J. Yang, X. L. Li, J. W. Zhou, B. Wang and J. L. Cheng, *Chinese J. Polym. Sci*., 38(2020)403.
7. J. Li, Y. Sun, J. Wang, J. Tian, X. Q. Zhang, H. Yang and B. P. Lin, *J. Alloys Compd.*, 749(2018)783.
8. C. Y. Hsu, J. Zhang, T. Sato, S. Moriyama and M. Higuchi, *ACS Appl. Mater. Interfaces*., 7(2015)18266.
9. J. Platt, *J. Chem. Phys.*, 34(1961)862.
10. Q. Chen, Y. Shi, K. Sheng, J. Zheng and C. Xu, *ACS Appl. Mater. Interfaces*., 13(2021)56544.

11. J. Chu, D. Lu, B. Wu, X. Wang, M. Gong, R. Zhang and S. Xiong, *Sol. Energy Mater Sol. Cells*., 177(2018)70.
12. S. Ming, H. Zhang, Y. Zhang, F. Jiang, K. Lin, G. X. J. Nie and J. Zhao, *Dyes Pigm.*, 198(2022)110010.
13. W. T. Neo, C. M. Cho, Z. Shi, S. T. Chua and J. Xu, *J. Mater. Chem. C*., 4(2016)28.
14. Y. Rao, J. Dai, C. Sui, Y. T. Lai, Z. Li, H. Fang, X. Li, W. Li and P. Hsu, *ACS Energy Lett.*, 6(2021)3906.
15. B. Zhuang, X. Wang, Q. Zhang, J. Liu, Y. Jin and H. Wang, *Sol. Energy Mater Sol. Cells.*, 232(2021)111357.
16. G. Wang, L. Zhang and J. Zhang, *Chem. Soc. Rev.,* 41(2012797.
17. P. Yang, P. Sun and W. Mai, *Mater. Today.*, 19(2016)394.
18. A. M. Bryan, L. M. Santino, Y. Lu, S. Acharya and J. M. D'Arcy, *Chem. Mater.,* 28(2016)5989.
19. X. Lu, M. Yu, G. Wang, Y. Tong and Y. Li, *Energy Environ. Sci.,* 7(2014)2160.
20. T. B. Schon, B. T. McAllister, P. F. Li and D. S. Seferos, *Chem. Soc. Rev.*, 45(2016)6345.
21. G. Inzelt, M. Pineri, J. W. Schultze and M. A. Vorotyntsev, *Electrochim. Acta.*, 45(2000)2403.
22. P. Simon, Y. Gogotsi, *Nat. Mater*., 7(2008)845.
23. Y. Zhang, S. Yu, G. Lou, Y. Shen, H. Chen, Z. Shen, S. Zhao, J. Zhang, S. Chai and Q. Zou, *J. Mater. Sci.,* 52(2017)11201.
24. S. Matsushita, B. Yan, T. Matsui, J. D. Kim and K. Akagi, *RSC Advances.*, 8(2018)19512.
25. X. Gao, Y. Dong, S. Li, J. Zhou, L. Wang and B. Wang, *Electrochemical Energy Reviews.*, 3(2020)81.
26. A. Laforgue and L. Robitaille, *Macromolecules.*, 43(2010)4194.
27. N. Wang, G. Han, H. Song, Y. Xiao, Y. Li, Y. Zhang and H. Wang, *J. Power Sources.*, 395(2018)228.
28. I. Zhitomirsky, M. Cheong and J. Wei, *JOM.*, 59(2007)66.
29. C. Gu, Y. Bao, W. Huang, D. Liu and R. Yang, *Chem. Phys.*, 217(2016)748.
30. Y. Wang, Y. Shi, L. Pan, Y. Ding, Y. Zhao, Y. Li, Y. Shi and G. Yu, *Nano Lett*., 15(2015)7736.
31. G. Nie, J. Xu, S. Zhang, T. Cai and X. Han, *J. Appl. Polym. Sci*., 102(2006)1877.
32. G. Sönmez and S. A. Sezai, *Synth Met*., 135-136(2003)459.
33. F. Wan, L. Li, X. Wan and G. Xue, *J. Appl. Polym. Sci*., 85(2002) 814.
34. S.W. Cai, H. L. Wen, S. Z. Wang, H. J. Niu, C. Wang, X. K. Jiang, X. D. Bai and W. Wang, *J. Electroanal. Chem*., 228(2017) 332.
35. L. L. Hench, and J. K. West, *Chem Rev*., 90(1990)33.
36. P. M. Beaujuge, and J. R. Reynolds, *Chem Rev*., 110(2010) 268.
37. X. Li, W. Wei, C. Zhang, M. Wei, D. R. Yu, and Q. Y. Zhu, *China's Ceramics*, 56(2020)9.
38. Q. Z. Pi, D. Q. Bi, D. F. Qiu, H. W. Wang, X. F. Cheng, Y. Q. Feng, Q. Zhao and M. D. Zhou, *J. Mater. Chem. C*., 9(2021) 8994.
39. Y. Sun, X. Zhao, G. Q. Zhu, M. Li, X. Q. Zhang, H. Yang and B. P. Lin, *Electrochim. Acta*., 333(2020) 135495.
40. Y. Zhang, L. Q. Kong, X. P. Ju, H. M. Du, J. S. Zhao, and Y. Xie, *RSC Advances*, 8(2018)21252.
41. W. J. Yoo, T. Tsukamoto, and S. Kobayashi, *Org Lett*., 17(2015) 3640.
42. P. N. Wang, Y. Sun, J. Li, W.W. Kang, G. Q. Zhu, H. J. Zhang, X. Q. Zhang, H. Yang and B. P. Lin, *New J Chem*., 45(2021) 18472.
43. J. J. Li, Q. F. Guo, Y. Lu and G. M. Nie, *J. Eur Polym J.*, 113(2019) 29.
44. L. Chen, H. R. Zhang, S. N. Liu, C. H. Sun, X. J. Hu and S. Y. Zhou, *J. Surf Interface Anal*., 52(2020) 389.
45. Z. Xu, M. Wang, W. Y. Fan, J. S. Zhao, and H. S. Wang, *Electrochim. Acta*.,160(2015)271.
46. C. Y. Gu, Y. Bao, W. Huang, D. Y. Liu and R. Q. Yang, *Macromol Chem Phys*., 217(2016) 748.
47. H. H. Zhang, Y. Zhang, C. Gu and Y. G. Ma, Adv. *Energy Mater.*, 5(2015) 1402175.
48. Q. Meng, K. Cai, Y. Chen and L. Chen, *Nano Energy*., 36(2017) 268.

49. Y. D. Zhang, J. F. Ding, W. Xu, M. Wang, R. Shao, Y. Sun and B. P. Lin, *Chem Eng J*., 386(2020) 124030.
50. S. H. Hsiao and J. C. Hsueh, J. *Electroanal. Chem*., 758(2015) 100.
51. A. Afif, S. M. H. Rahman, A. A. Tasfiah, J. Zaini, M. A. Islan and A. K. Azad, *J Energy Storage*.,25(2019) 100852.
52. M. M. Yu, X. W. Ji and F. Ran, *Carbohydr Polym*.,255(2021)117346.
53. J. Liu, Z. Wang, Q. Liu, S. R. Li, D. C. Wang and Z. F. Zheng, *Chem. Eng. J*.,447(2022) 137562.
54. L. Tang, Z. K. Yang, F. Duan and M. Q. Chen, *J Mater Sci-Mater El.*,28(2017)15804.
55. L. Tang, F. Duan and M. Q. Chen, *J Solid State Electrochem*.,20(2016)2805.
56. H. G. Wei, H. B. Gu, J. Guo. S. Y. Wei, J. R. Liu and Z. H. Guo, *J. Phys. Chem. C*., 25(117)13000.
57. X. Y. Chen, P. Chang, S. Zhang, L. X. Guan, G. H. Ren and J. G. Tao, *Nanotechnology*, 33(2021) 085403.
58. G. Q. Zhu, Y. Sun, M. Li, C. X. Tao, X. Q. Zhang, H. Yang, L. X. Guo and B. P. Lin, *Electrochim. Acta*.,365(2021)137373.
59. D. K. Fong, T. S. Wang, H. K. Kim, R. V. Kumar and S. K. Amoukov, *ACS Energy Lett*., 2(2017)2014.
60. X. C. Li, Y. Z. Zhang, C. Y. Wang, Y. Wan, W. Y. Lai, H. Pang and W. Huang, *Chem. Sci*.,8(2017)2959.